Flexible Organic Light-Emitting Diodes with Improved Outcoupling Efficiency

Changyeong Jeong, Yong-Bum Park, and L. Jay Guo
Electrical Engineering and Computer Science, University of Michigan, Ann Arbor, MI, USA

Abstract

We developed dielectric-metal-dielectric (DMD) anode to reduce both rigidity and reflectivity of the film. With optimization of DMD considering adjacent layers used in real devices, we showed that flexible organic light-emitting diodes (OLEDs) made on DMD can outperform conventional OLEDs made on ITO.

Author Keywords

OLEDs; thin metal films; FTCs; high transmittance; Antireflection coatings; flexible OLEDs; green OLEDs.

1. Objective and Background

There has been significant increase in demands of flexible displays in the market today. In this respect, organic light-emitting diodes (OLEDs) have great potential for future flexible displays and lightings since organic semiconductors are less expensive, easy to process, and intrinsically flexible due to Van der Waals bonding (1).

It is essential to find an appropriate conductor that is flexible and highly transmissive with low sheet resistance. ITO used in the conventional OLEDs is highly transparent but lacks in its flexibility (2). For this reason, there is a strong demands of high performance flexible transparent conductors (FTCs) that could successfully transform flexible technology to market (3-5).

Previously introduced flexible conductors like metal mesh, metal nanowires, graphene, etc, have not shown comparable optical or electrical properties when they are used to replace ITO in OLEDs (6-9). Dielectric-metal-dielectric (DMD) based FTCs shows one of the highest figure-of-merit among a variety of FTCs, indicating its great potential for flexible optoelectronic device application (10). Also, the simplicity in process fabrication and compatibility with existing display technology makes it an excellent candidate for immediate use in industry. Especially the ultrasmooth surface of the DMD makes it ideally suited for the thin-film based OLED structures. In this regard, the use of Cu-doped Ag (CuAg) is important to guarantee a continuous nm thick Ag layer with smooth morphology (10). For these reasons, DMD based FTC has been prevalently researched for various optoelectronic applications including organic photovoltaics, OLEDs, photodetectors, and so on (11-15).

Most reports so far focused primarily on optimizing the DMD with both sides in air, but not optimized with materials of the adjacent layers used in their corresponding applications. For high performance OLED, the layers in DMD stack need to be carefully designed and optimized by taking into account all the existing layers for OLED, especially the layers immediately on top and beneath the DMD.

In this work, we conducted optimization of DMD with the above consideration and show that the optimum design for DMD used in OLED is different from that DMD in air. By this deliberate design of DMD, we demonstrate that the OLEDs using DMD electrode can outperform ITO-based counterparts. Moreover, we show that DMD based OLED on a flexible substrate can be bended to 2 mm radius of curvature and maintain normal operation. This work demonstrates that DMD is a good candidate to replace ITO for future flexible displays.

2. Results and Discussion

Optimization of DMD based FTC: Optical simulation of ITO-CuAg-ITO based DMD optimization was conducted using transfer-matrix method (TMM). Complex refractive index values (*n-k*) of each optical layer used in the simulation were measured using Woollam M-2000 spectroscopic ellipsometer. Figure 1 (a) and (b) shows 2-dimensional (2D) color map of average transmittance (*T*) over green emission wavelength (430 – 630 nm) while varying the top and bottom ITO dielectric for DMD in air and embedded into OLED device, respectively.

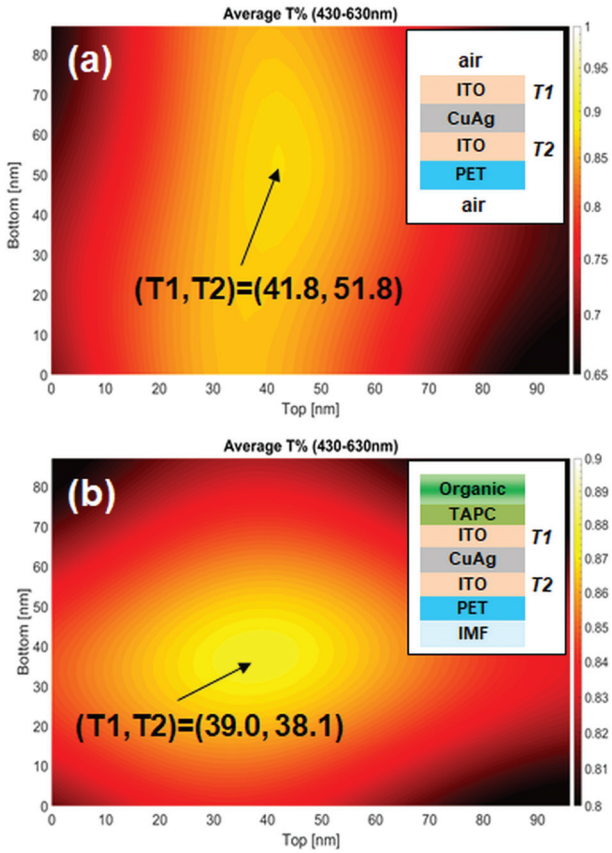

Figure 1. 2D colormap of average transmittance with varying top and bottom ITO dielectric thickness for DMD with (a) air-suspended and (b) embedded into OLED case

For the calculation, the top and bottom ITO dielectric's thickness indicated as T1 and T2 were varied from 0 to 90 nm while fixing Cu-Ag metal film thickness as 8 nm. The inset schematic in each colormap shows the optical stack structure

used in the simulation. In the case of DMD-substrate in air medium, the 2D map shows that the optimum top and bottom ITO dielectric thickness with highest transmission *T* at green wavelength resides at T1 = 41.8 nm and T2 = 51.8 nm. For the case of DMD inside OLED structure, *T* is the effective transmittance of light path from the emission layer (EML) through hole transport layer (HTL), MoO_x injection layer, TC, and to the substrate. the bottom medium was replaced by the index matching layer to the substrate. This is because, in practice, scatterer or microlens are used at the interface of the substrate to extract the light that is trapped at the substrate thereby maximizing the overall light extraction (16-20). For this case of having top medium as organic layer and bottom medium as medium with same index as the substrate, the optimum thickness resides at T1 = 39.0 nm and T2 = 38.1 nm. Note the significant difference in T2 in achieving maximum *T* in these two cases, which is related to the use of index matching layer underneath the substrate.

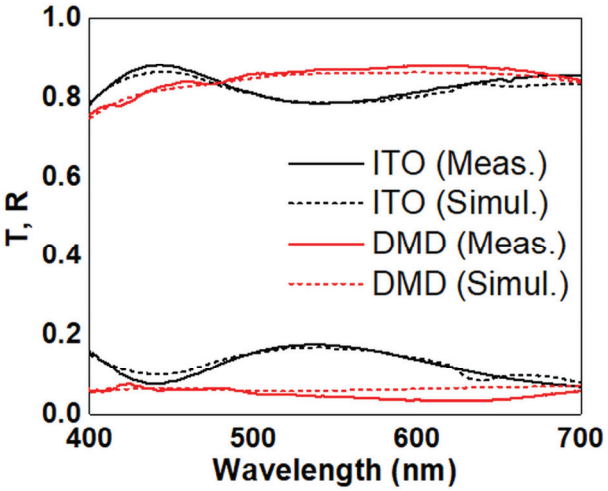

Figure 2. Transmittance (*T*) and reflectance (*R*) of DMD as a function of wavelength. Solid and dotted lines show measured and simulated *T* and *R*, respectively.

Figure 2 shows *T* and reflectance (*R*) of commercial ITO sample and fabricated DMD on a substrate based on optimum design from Figure 1 (b). Simulation spectra of these are also plotted in dotted lines. The measured electrical sheet resistance of the DMD and ITO are 12.8 and 10.0 Ω/sq, respectively.

Angle dependent reflectance: One argument which may weaken the metal-based DMD FTC over the traditional ITO counterparts is that metal films are known to be very reflective and the reflection can get aggravated especially at a large angle of incidence. To verify this point, simulation of TMM for angle of incidence range from 0 to 80° was calculated for ITO and DMD and shown in Figure 3 (a) and (b), respectively. Surprisingly, the simulation results show that metal-based DMD TC shows lower *R* intensity compared to ITO even up to 80° angle of incidence. This can be understood in the context of the top and bottom dielectric layers in DMD serving as anti-reflective coating layers by inducing destructive interference for the reflected light.

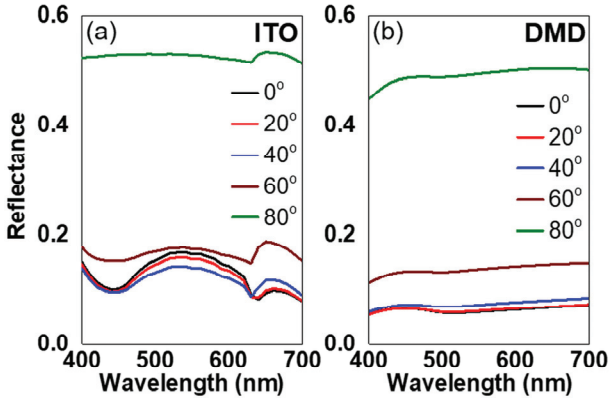

Figure 3. Simulated angle dependent reflectances of (a) ITO and (b) DMD films as functions of wavelength.

OLEDs performances: We fabricated OLEDs with anode made of DMD designed in the previous sections. Figure 4 (a) shows a device structure of the fabricated OLEDs. A device with conventional ITO anode is used as the control. The ITO device was made on a glass substrate, whereas the DMD device on a PET substrate since the DMD device is highly flexible and emit light under bending. MoO_x and LiF are hole and electron injection layers, respectively, and TAPC and TPBi are hole and electron transporting layers, respectively. Emissive layer consists of 10% $Ir(ppy)_2acac$ doped in CBP. Since the top dielectric of DMD is ITO, electrical injection property for both devices are identical.

Figure 4 (b) shows EQE of the ITO and DMD devices with and without the index matching fluid (IMF). As shown, the ITO and DMD devices show very similar EQEs without IMF, but EQE of the DMD device becomes higher with IMF. It means that more photons are trapped in the DMD device than the ITO device.

The efficiency enhancement of the DMD device can be understood in two ways. First, DMD has lower reflectance than ITO as shown in Figure 2 and 3. Therefore, more generated photons can pass through the anode and escape out of the device with IMF. Also, the waveguide mode formed in the DMD OLEDs is more loosely confined than the ITO device, which implies that more photons can be extracted from the substrate by using IMF.

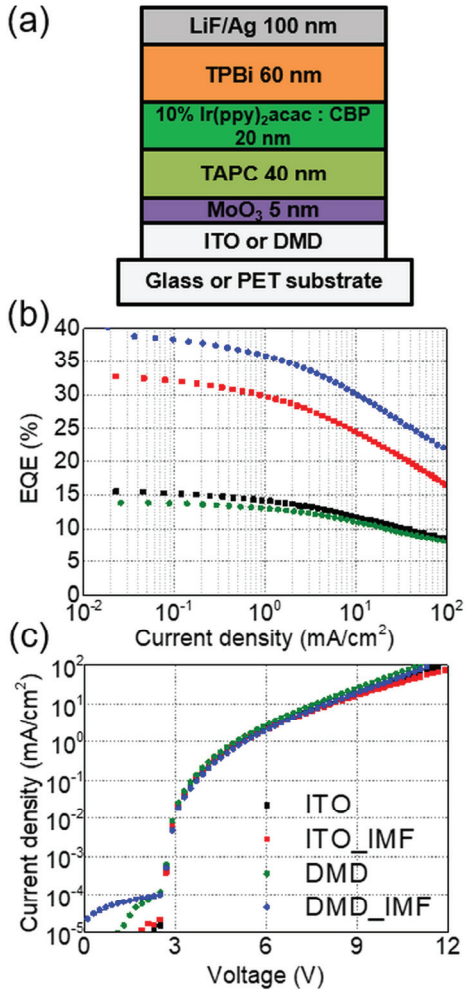

Figure 4. (a) Device structure of OLEDs made in this work. (b) External quantum efficiency (EQE) and (c) current density-voltage (*J-V*) characteristics of control and DMD devices with and without index-matching fluid (IMF).

The measured current density (J) versus applied voltage (V) for the ITO and DMD devices is plotted in Figure 4 (c), and they have very similar behaviors. It is because DMD and ITO have comparable sheet resistances and ITO is the top dielectric layer in the DMD, indicating that workfunction of the anode for both devices are the same.

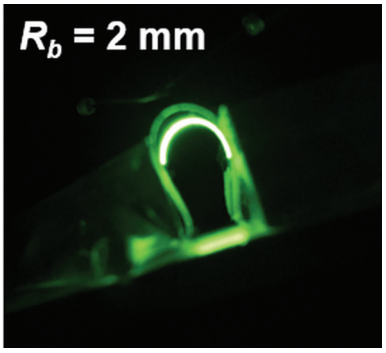

Figure 5. Picture of the fabricated DMD device with the bending radius (R_b) of 2 mm under operation. Light emission from the device area is observable.

The DMD device is highly flexible since rigid ITO is replaced with DMD. Figure 5 shows the bended DMD sample with bended radius (R_b) = 2 mm. We tested that the sample is continuously illuminating from the large R_b to 2 mm. Significantly small R_b shines the light on great potential of DMD over ITO.

Angle insensitivity: Since the DMD device includes 8 nm Ag layer in the middle, there could be concern over the angle sensitivity of the device emission spectra due to possible stronger optical cavity effect in the OLED structure. Figure 6 shows angle dependent emission profile of both the ITO and DMD devices. The DMD device also shows Lambertian-like emission profile, indicating that it does not have strong cavity effect. Again, this can be attributed to the overall lower reflectance of the DMD structure by virtue of anti-reflection offered by the optimized dielectric layer thickness.

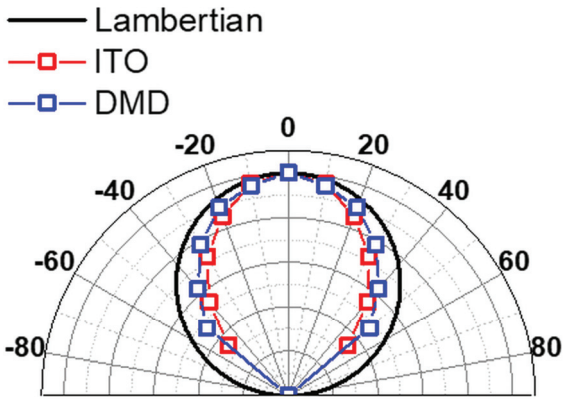

Figure 6. Measured angle dependent emission profiles. Both the ITO and DMD OLEDs show emission profiles like Lambertian.

Figure 7 show spectra of the devices measured at oblique angles. The spectra of the DMD device do not change much with angle, which is another evidence for the angle insensitivity of the DMD device.

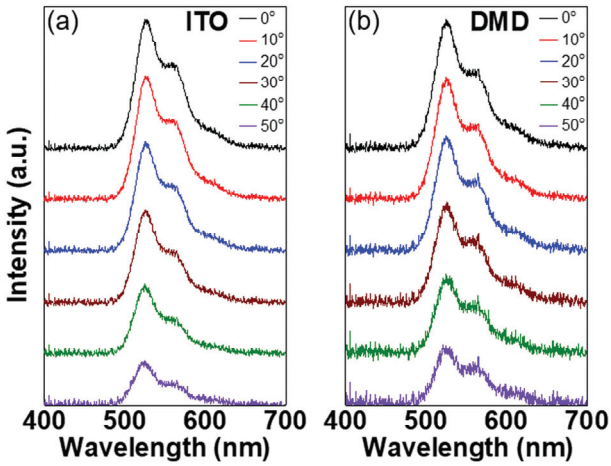

Figure 7. Measured angle dependent spectra of (a) ITO and (b) DMD devices.

Figure 8 shows CIE coordinate change with the measured angles. Spectra in Figure 7 were used to calculate the CIE coordinates.

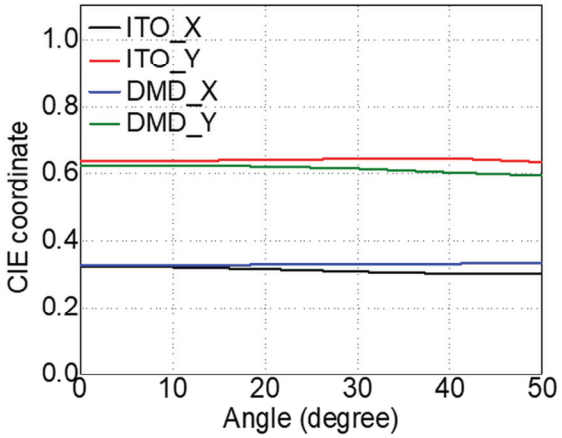

Figure 8. CIE coordinate changes as a function of the measured angle of the ITO and DMD devices.

Both *x* and *y* coordinates of the two devices do not change much with angles, meaning that Ag placed in the middle of DMD does not have strong reflection.

3. Conclusion

The ITO-based DMD (ITO-CuAg-ITO) has similar optical and electrical properties with ITO. We demonstrated that OLEDs with DMD outperforms that with ITO in terms of efficiency with almost the identical *J-V* characteristics and spectral change in this work. DMD OLEDs can still operate at R_b = 2 mm and showed consistent spectra at oblique angles without any spectral distortion, indicating that the layered dielectrics of DMD compensate reflections from the Ag layer. Therefore, this work shows that DMD can certainly be an option for the ITO replacement since it is almost the same film with ITO but highly improved flexibility.

4. Impact

This work shows that flexible OLEDs can outperform conventional ITO-based OLEDs. DMD developed in our group is comparable to commercial ITO in optical and electrical properties, but additionally it has high flexibility. DMD can be an excellent replacement of ITO in the future display and lightings.

5. Acknowledgements

We would like to acknowledge the support by the MTRAC program.

6. References

1. Forrest SR. The path to ubiquitous and low-cost organic electronic appliances on plastic. Nature. 2004;428(6986):911-8.
2. Sierros KA, Morris NJ, Ramji K, Cairns DR. Stress–corrosion cracking of indium tin oxide coated polyethylene terephthalate for flexible optoelectronic devices. Thin Solid Films. 2009;517(8):2590-5.
3. Song T-B, Li N. Emerging Transparent Conducting Electrodes for Organic Light Emitting Diodes. Electronics. 2014;3(1):190-204.
4. Park MH, Han TH, Kim YH, Jeong SH, Lee Y, Seo HK, et al. Flexible organic light-emitting diodes for solid-state lighting. J Photon Energy. 2015;5.
5. Morales-Masis M, De Wolf S, Woods-Robinson R, Ager JW, Ballif C. Transparent Electrodes for Efficient Optoelectronics. Advanced Electronic Materials. 2017;3(5).
6. Han T-H, Lee Y, Choi M-R, Woo S-H, Bae S-H, Hong BH, et al. Extremely efficient flexible organic light-emitting diodes with modified graphene anode. Nature Photonics. 2012;6(2):105-10.
7. Kim J, Ganorkar S, Kim Y-H, Kim S-I. Graphene oxide hole injection layer for high-efficiency polymer light-emitting diodes by using electrophoretic deposition and electrical reduction. Carbon. 2015;94:633-40.
8. Chen D, Zhao F, Tong K, Saldanha G, Liu C, Pei Q. Mitigation of Electrical Failure of Silver Nanowires under Current Flow and the Application for Long Lifetime Organic Light-Emitting Diodes. Advanced Electronic Materials. 2016;2(8).
9. Liang G, Hu H, Liao L, He Y, Ye C. Highly Flexible and Bright Electroluminescent Devices Based on Ag Nanowire Electrodes and Top-Emission Structure. Advanced Electronic Materials. 2017;3(3).
10. Zhang C, Kinsey N, Chen L, Ji C, Xu M, Ferrera M, et al. High-Performance Doped Silver Films: Overcoming Fundamental Material Limits for Nanophotonic Applications. Adv Mater. 2017;29(19).
11. Kim S, Lee JL. Design of dielectric/metal/dielectric transparent electrodes for flexible electronics. J Photon Energy. 2012;2.
12. Kim S, Yu HK, Hong K, Kim K, Son JH, Lee I, et al. MgO nano-facet embedded silver-based dielectric/metal/dielectric transparent electrode. Opt Express. 2012;20(2):845-53.
13. Cattin L, Bernède JC, Morsli M. Toward indium-free optoelectronic devices: Dielectric/metal/dielectric alternative transparent conductive electrode in organic photovoltaic cells. physica status solidi (a). 2013;210(6):1047-61.
14. Kim H, Lee K-T, Zhao C, Guo LJ, Kanicki J. Top illuminated organic photodetectors with dielectric/metal/dielectric transparent anode. Organic Electronics. 2015;20:103-11.
15. Liu S-W, Su T-H, Chang P-C, Yeh T-H, Li Y-Z, Huang L-J, et al. ITO-free, efficient, and inverted phosphorescent organic light-emitting diodes using a WO 3 /Ag/WO 3 multilayer electrode. Organic Electronics. 2016;31:240-6.
16. Sun Y, Forrest SR. Organic light emitting devices with enhanced outcoupling via microlenses fabricated by imprint lithography. Journal of Applied Physics. 2006;100(7).
17. Sun Y, Forrest SR. Enhanced light out-coupling of organic light-emitting devices using embedded low-index grids. Nature Photonics. 2008;2(8):483-7.
18. Qu Y, Slootsky M, Forrest SR. Enhanced light extraction from organic light-emitting devices using a sub-anode grid. Nature Photonics. 2015;9(11):758-63.
19. Koh T-W, Spechler JA, Lee KM, Arnold CB, Rand BP. Enhanced Outcoupling in Organic Light-Emitting Diodes via a High-Index Contrast Scattering Layer. ACS Photonics. 2015;2(9):1366-72.
20. Lee KM, Fardel R, Zhao L, Arnold CB, Rand BP. Enhanced outcoupling in flexible organic light-emitting diodes on scattering polyimide substrates. Organic Electronics. 2017;51:471-6.